



Simultaneous Voltammetric Determination of Ascorbic Acid and Uric Acid Using a Modified Multiwalled Carbon Nanotube Paste Electrode

Hadi Beitollahi^a, Hassan Karimi-Maleh^b, Iran Sheikhshoae^c

^a *Environment Department, International Center for Science, High Technology & Environmental Sciences, Kerman, Iran*

^b *Department of Chemistry, Science and Research Branch, Islamic Azad University, Mazandaran, Iran*

^c *Department of Chemistry, Faculty of Science, Shahid Bahonar University of Kerman, Kerman 76175-133, Iran*

* Corresponding author: E-mail address: h.beitollahi@yahoo.com

Received 12 December 2011 | Received in revised form 6 March 2012 | Accepted 22 April 2012

Abstract: This paper describes the development, electrochemical characterization and utilization of novel modified molybdenum (VI) complex-carbon nanotube paste electrode for the electrocatalytic determination of ascorbic acid (AA). The electrochemical profile of the proposed modified electrode was analyzed by cyclic voltammetry (CV) that showed a shift of the oxidation peak potential of AA about 235 mV to less positive value, compared with an unmodified carbon paste electrode. Differential pulse voltammetry (DPV) in 0.1 M phosphate buffer solution (PBS) at pH 7.0 was performed to determine AA in the range of 0.1 to 950.0 μ M, with a detection limit of 89.0 nM. Then the modified electrode was used to determine AA in an excess of uric acid (UA) by DPV. Finally, this method was used for the determination of AA in some real samples.

Key words: Ascorbic acid, Uric acid, Carbon nanotubes, Modified electrode, Electrocatalysis

©2012 Published by University of Mazandaran. All rights reserved.

1. Introduction

Ascorbic acid (AA) and uric acid (UA) are both present in most of the biological fluids (plasma, serum, urine, tears, cerebrospinal fluids). At physiological levels, AA is a powerful water soluble antioxidant. It plays a key role in protecting living cells against oxidative injury and has been used clinically for the treatment and prevention of scurvy, common cold, mental illness, cancer and AIDS [1–3]. In the reverse, extreme AA levels can cause gastric

irritation, diarrhea and renal problems [1]. The role of UA in conditions associated with oxidative stress is not entirely clear. While commonly regarded as an indicator of gout, epidemiological studies suggest that high UA levels in serum represent a risk factor for cardiovascular diseases [4], UA stones [5] and Lesch–Nyhan syndrome [6]. Both AA and UA are useful in the monitoring of oxidative stress and moreover may be considered as biochemical markers in a lot of pathologies (neonatal hypoxia, coronary heart diseases . . .). Thus the selective and convenient

detection of AA and UA is very important for biological researches as well as for routine analysis. This explains the numerous methods dedicated to their qualitative and quantitative determination.

Usual procedures for the quantitative determination of AA and UA are generally based on enzymatic methods [7], spectrofluorometry [8], HPLC analysis [9] or capillary electrophoresis [3]. However these methods suffer from costly materials and complex experimental protocols, require sample pretreatment and are generally time consuming. In the last two decades, electrochemical procedures have been greatly employed due to their advantages such as simplicity, low cost, fast analysis and good selectivity [10]. However, a major problem is that AA and UA require generally high overpotentials on usual non-modified bare electrodes. Furthermore both acids are in these conditions oxidized at very close potentials which make their simultaneous detection and quantitative determination difficult [11]. Various approaches have been attempted to solve these problems. Chemically modified electrodes have been particularly developed to discriminate between the electrochemical responses of AA and UA oxidation. Several electrode modification processes have been tested [12-20]

Carbon paste electrode (CPE) is a special kind of heterogeneous carbon electrode consisting of mixture prepared from carbon powder (as graphite, glassy carbon and others carbonaceous materials) and a suitable water-immiscible or non-conducting binder [20-24]. The use of carbon paste as an electrode was initially reported in 1958 by Adams [26].

In afterward researches a wide variety of modifiers have been used with these versatile electrodes such as ferrocene and its derivatives, metal oxides, enzymes

and etc. [27-33]. CPEs are widely applicable in both electrochemical studies and electroanalysis thank to their advantages such as very low background current (compared to solid graphite or noble metal electrodes), facility to prepare, low cost, large potential window, simple surface renewal process and easiness of miniaturization.

Besides the advantageous properties and characteristics listed before, the feasibility of incorporation different substances during the paste preparation (which resulting in the so-called modified carbon paste electrode), allow the fabrication of electrodes with desired composition, and hence, with pre-determined properties [33-41].

Since the discovery of carbon nanotubes (CNTs) in 1991 [42], numerous investigations were focused on the studies of their properties and applications [43, 44]. Because of the special tube structure, CNTs possess several unique properties such as good electrical conductivity, high chemical stability and extremely high mechanical strength [45]. In addition, the subtle electronic behavior of CNTs reveals that they have the ability to promote electron-transfer reaction and have a high electrocatalytic effect when used as electrode materials. All these fascinating properties make CNTs as a suitable candidate for the modification of electrodes [46-50].

Thus, in this paper, we described initially the preparation and suitability of a molybdenum (VI) complex-modified carbon nanotube paste electrode (MC-CNPE) as a new electrode in the electrocatalysis and determination of AA in an aqueous buffer solution, then we evaluated the analytical performance of the modified electrode in quantification of AA in the presence of UA.

2. Experimental

2.1. Apparatus and materials

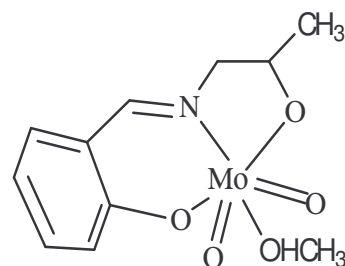
The electrochemical measurements were performed with an Autolab potentiostat/galvanostat (PGSTAT 12, Eco Chemie, the Netherlands). The experimental conditions were controlled with General Purpose Electrochemical System (GPES) software. A conventional three electrode cell was used at 25 ± 1 °C. An Ag/AgCl/KCl (3.0 M) electrode, a platinum wire, and the molybdenum (VI) complex-carbon nanotube paste electrode (MC-CNPE) were used as the reference, auxiliary and working electrodes, respectively.

A Metrohm 691 pH/Ion Meter was used for pH measurements. The prepared electrodes were characterized by scanning electron microscopy (SEM), Philips, Model XLC. All solutions were freshly prepared with double distilled water. AA, UA and all other reagents were of analytical grade from Merck (Darmstadt, Germany). Graphite powder and paraffin oil (DC 350, density = 0.88 g cm^{-3}) as the binding agent (both from Merck) were used for preparing the pastes.

Multiwalled carbon nanotubes (purity more than 95%) with o.d. between 10 and 20 nm, i.d. between 5 and 10 nm, and tube length from 0.5 to 200 μm were prepared from Nanostructured & Amorphous Materials, Inc. The 0.1 M phosphate buffer solutions (PBS) were prepared from orthophosphoric acid and its salts in the pH range of 2.0-11.0. Molybdenum(VI) complex (Scheme 1) was synthesized in our laboratory as reported previously [51].

2.2. Preparation of the electrode

The MC-CNPEs were prepared by hand mixing 0.01 g of MC with 0.89 g graphite powder and 0.1 g CNTs with a mortar and pestle. Then, $\sim 0.7 \text{ mL}$ of paraffin was added to the above mixture and mixed for 20 min until a uniformly-wetted paste was obtained. The paste was then packed into the end of a glass tube (ca. 3.4 mm i.d. and 10 cm long).



Scheme 1. Structure of dioxo-molybdenum (VI) complex $[\text{MoO}_2(\text{L})(\text{CH}_3\text{OH})]$

A copper wire inserted into the carbon paste provided the electrical contact. When necessary, a new surface was obtained by pushing an excess of the paste out of the tube and polishing with a weighing paper.

For comparison, MC modified CPE electrode (MC-CPE) without CNTs, CNT paste electrode (CNPE) without MC, and unmodified CPE in the absence of both MC and CNTs were also prepared in the same way.

3. Results and discussion

3.1. SEM Characterization

Typical SEM images of different electrodes were shown in Fig. 1. Fig. 1A shows the layer of irregularly flakes of graphite powder present on the surface of CPE. After multiwall carbon nanotubes added to the carbon paste, it can be seen that CNTs

were distributed on the paste (Fig. 1B). Fig. 1C shows that MC plus CNTs dispersed in the modified electrode.

3.2. Electrochemical properties of modified MC-CNPE

To the best of our knowledge there is no prior report on the electrochemical properties and, in particular, the electrocatalytic activity of MC in aqueous media. Therefore, we prepared MC-CNPE and studied its electrochemical properties in PBS (pH 7.0) using CV. It should be noted that one of the advantages of MC as an electrode modifier is its insolubility in aqueous media. Experimental results showed

reproducible, well-defined, anodic and cathodic peaks with E_{pa} , E_{pc} and $E^{\circ'}$ of 0.325, 0.235 and 0.28 V vs. Ag/AgCl/KCl (3.0 M), respectively. The observed peak separation potential, $\Delta E_p = (E_{pa} - E_{pc})$ of 90 mV, was greater than the value of $59/n$ mV expected for a reversible system [52], suggesting that the redox couple of MC in MC-CNPE has a quasi-reversible behavior in aqueous medium. The effect of the potential scan rate (v) on electrochemical properties of the MC-CNPE was also studied by CV (Fig. 2). Plots of the both anodic and cathodic peak currents (I_p) were linearly dependent on v in the range of 10 to 1000 mV s^{-1} (Fig. 2A), indicating that the redox process of MC at the modified electrode is diffusionless in nature [52].

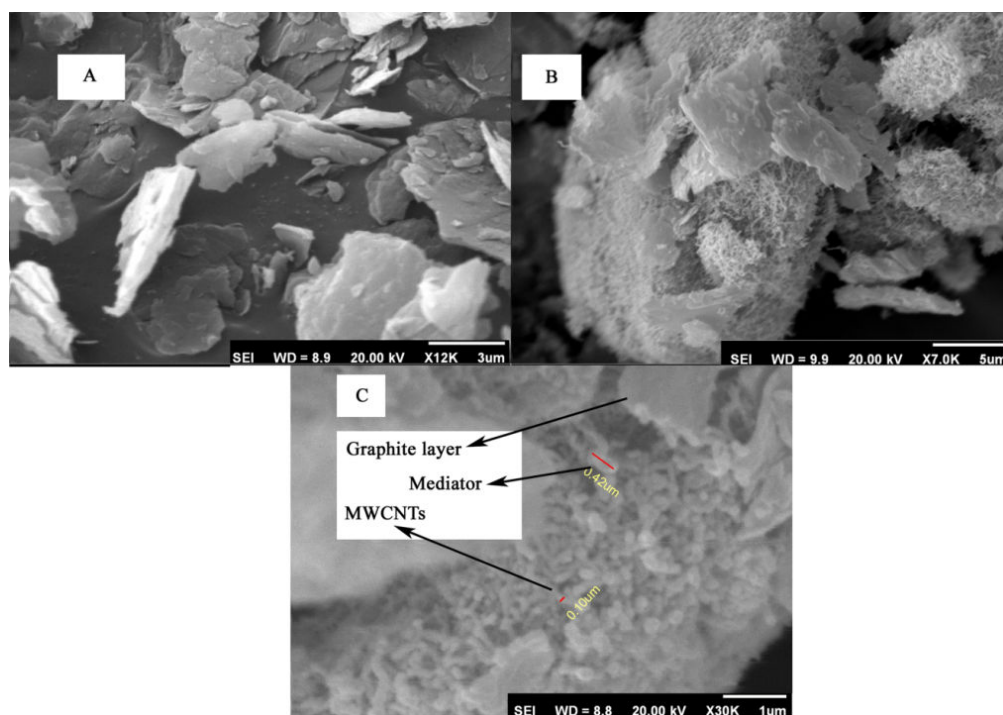


Fig. 1. SEM images of A) CPE, B) CNPE, and C) MC-CNPE.

The apparent charge transfer rate constant, k_s , and the charge transfer coefficient, α , of a surface-confined redox couple can be evaluated from CV experiments by using the variation of anodic and cathodic peak potentials with logarithm of scan rate, according to the procedure of Laviron [53]. Fig. 2B shows such plots, indicating that the E_p values are proportional to the logarithm of scan rate for v values higher than 5 V s^{-1} (Fig. 2C). The slopes of the plots in Fig. 2C can be used to extract the kinetic parameters α_c and α_a (cathodic and anodic transfer coefficients, respectively). The slope of the linear segments are equal to $-2.303RT/\alpha nF$ and $2.303RT/(1 - \alpha)nF$ for

the cathodic and anodic peaks, respectively. The evaluated value for the α is 0.5. Also, eq. 1 can be used to determine the electron transfer rate constant between modifier (MC) and CNPE:

$$\log k_s = \alpha \log (1-\alpha) + (1-\alpha) \log \alpha - \log (RT/nFv) - \alpha (1-\alpha) nF\Delta E_p/2.3RT \quad (1)$$

where $(1-\alpha)n_a = 0.5$, v is the sweep rate. All other symbols have their conventional meanings. The value of k_s was evaluated to be 24.6 s^{-1} using eq. (1).

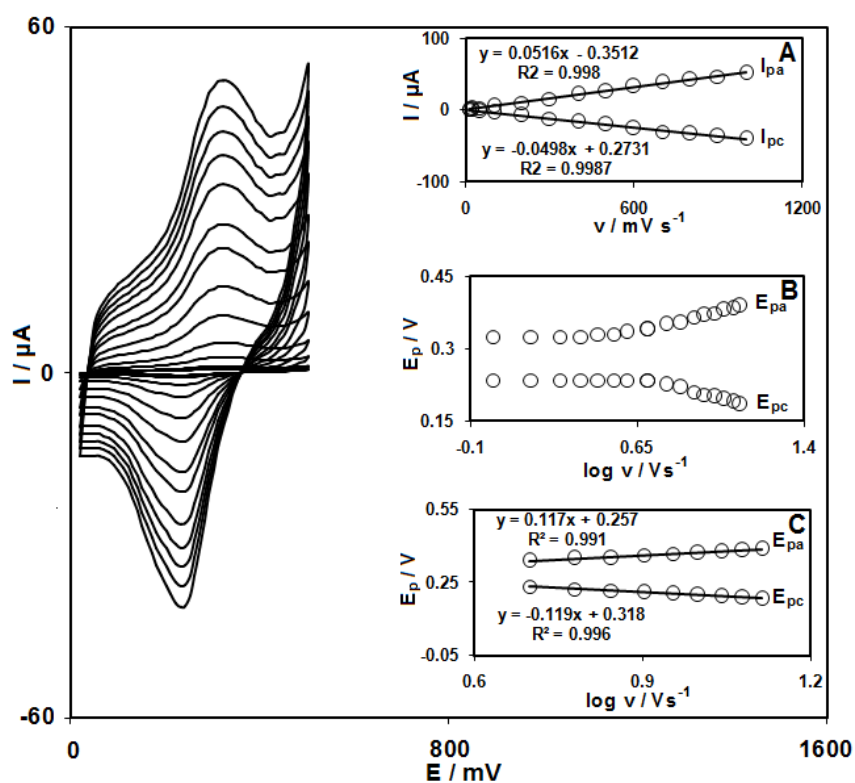


Fig. 2. CVs of MC-CNPE in 0.1 M PBS (pH 7.0), at various scan rates, from inner to outer, 10, 20, 50, 100, 200, 300, 400, 500, 600, 700, 800, 900 and 1000 mV s^{-1} . Insets: (A) Variations of I_p versus different scan rates: 10, 20, 50, 100, 200, 300, 400, 500, 600, 700, 800, 900 and 1000 mV^{-1} . (B) Variation of E_p vs. the logarithm of scan rates; (C) Variation of E_p versus the logarithm of the high scan rates.

3.3. Electrocatalytic oxidation of AA at MC-CNPE

Fig. 3 depicts the CV responses for the electrochemical oxidation of 0.1 mM AA at unmodified CPE (curve b), CNPE (curve d), MC-CPE (curve e) and MC-CNPE (curve f). As it is seen, while the anodic peak potential for AA oxidation at the CNPE, and unmodified CPE are 500 and 560 mV, respectively, the corresponding potential at MC-CNPE and MC-CPE is ~ 325 mV. These results indicate that the peak potential for AA oxidation at the MC-CNPE and MC-CPE electrodes shift by ~ 175 and 235 mV toward negative values compared to CNPE and unmodified CPE, respectively. However, MC-CNPE shows much higher anodic peak current for the oxidation of AA compared to MC-CPE,

indicating that the combination of CNTs and the mediator (MC) has significantly improved the performance of the electrode toward AA oxidation. In fact, MC-CNPE in the absence of AA exhibited a well-behaved redox reaction (Fig.3, curve c) in 0.1 M PBS (pH 7.0). However, there was a drastic increase in the anodic peak current in the presence of 0.1 mM AA (curve f), which can be related to the strong electrocatalytic effect of the MC-CNPE towards this compound [43].

This value is comparable with values reported by other research groups for electrocatalytic oxidation of AA at the surface of chemically modified electrodes by other mediators (Table 1).

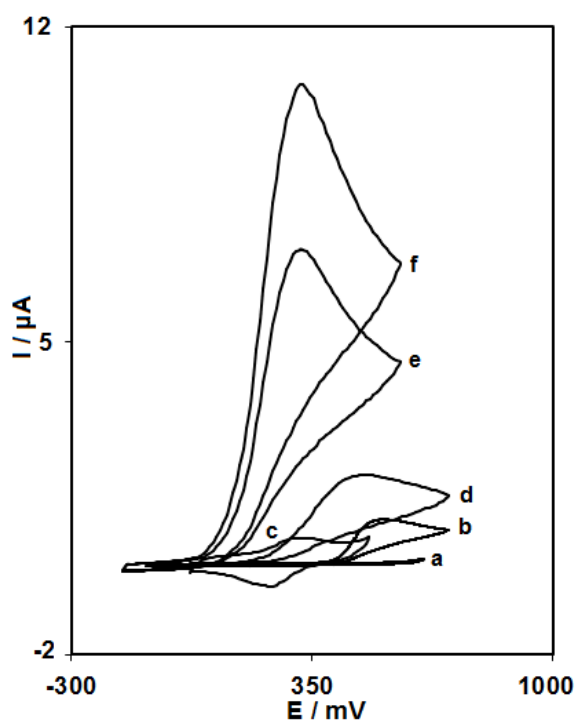


Fig. 3. CVs of (a) unmodified CPE in 0.1 M PBS (pH 7.0) at scan rate of 10 mV s^{-1} ; (b) as (a) + 0.1 mM AA; (c) as (a) at the surface of MC-CNPE; (d) as (b) at the surface of CNPE; (e) as (b) at the surface of MC-CPE; (f) as (b) at the surface of MC-CNPE.

Table1. Comparison of the efficiency of some modified electrodes used in the electrocatalysis of AA.

Electrode	Modifier	pH	Peak potential shift (mV)	Scan rate (mV/s)	LOD (M)	LDR (M)	Ref.
Carbon paste	2,7-Bis(ferrocenyl ethyl)fluoren-9-one	7.0	300	10	9.0×10^{-6}	3.1×10^{-5} – 3.3×10^{-3}	10
Carbon paste	2, 2'-[1, 2-ethanediybis (nitriloethylidyne)]-bis-hydroquinone	7.0	380	10	7.5×10^{-8}	1.0×10^{-7} – 8.0×10^{-4}	12
Carbon paste	Bis(40-(4-pyridyl)-2,20:60,200-terpyridine)iron(II) thiocyanate	5.0	200	100	2.0×10^{-6}	3.88×10^{-6} – – 2.92×10^{-3}	34
Carbon paste	Molybdenum(VI) complex	7.0	235	10	8.9×10^{-8}	1.0×10^{-7} – 9.5×10^{-4}	This work

The effect of scan rate on the electrocatalytic oxidation of AA at the MC-CNPE was investigated by CV (Fig. 4). Results showed that the oxidation peak potential shifted to more positive potentials with increasing scan rate, confirming the kinetic limitation in the electrochemical reaction. Also, a plot of peak height (I_p) vs. the square root of scan rate ($v^{1/2}$) was found to be linear in the range of 10–60 mV s^{-1} , suggesting that, at sufficient overpotential, the process is diffusion rather than surface controlled (Fig. 4A). A plot of the scan rate-normalized current ($I_p/v^{1/2}$) vs. scan rate (Fig. 4B) exhibits the characteristic shape typical of an EC' process [50].

Fig. 4C, shows a Tafel plot that was drawn from data of the rising part of the current–voltage curve recorded at a scan rate of 10 mV s^{-1} . This part of voltammogram, known as Tafel region, is affected by electron transfer kinetics between substrate (AA) and surface confined MC, assuming the deprotonation of substrate as a sufficiently fast step. In this condition, the number of electron involved in the rate determining step can be estimated from the slope of

Tafel plot. A slope 0.084 V is obtained indicating a one electron transfer to be rate limiting step assuming a transfer coefficient of $\alpha = 0.3$.

3.4. Chronoamperometric measurements

Chronoamperometric measurements of AA at MC-CNPE were carried out by setting the working electrode potential at 0.4 V (at the first potential step) and at 0 V (at second potential step) vs. Ag/AgCl/KCl (3.0 M) for the various concentration of AA in PBS (pH 7.0) (Fig.5). For an electroactive material (AA in this case) with a diffusion coefficient of D, the current observed for the electrochemical reaction at the mass transport limited condition is described by the Cottrell equation [52]. Experimental plots of I vs. $t^{-1/2}$ were employed, with the best fits for different concentrations of AA (Fig. 5A).

The slopes of the resulting straight lines were then plotted vs. AA concentration (Fig. 5B). From the resulting slope and Cottrell equation the mean value of the D was found to be $4.23 \times 10^{-6} \text{ cm}^2/\text{s}$.

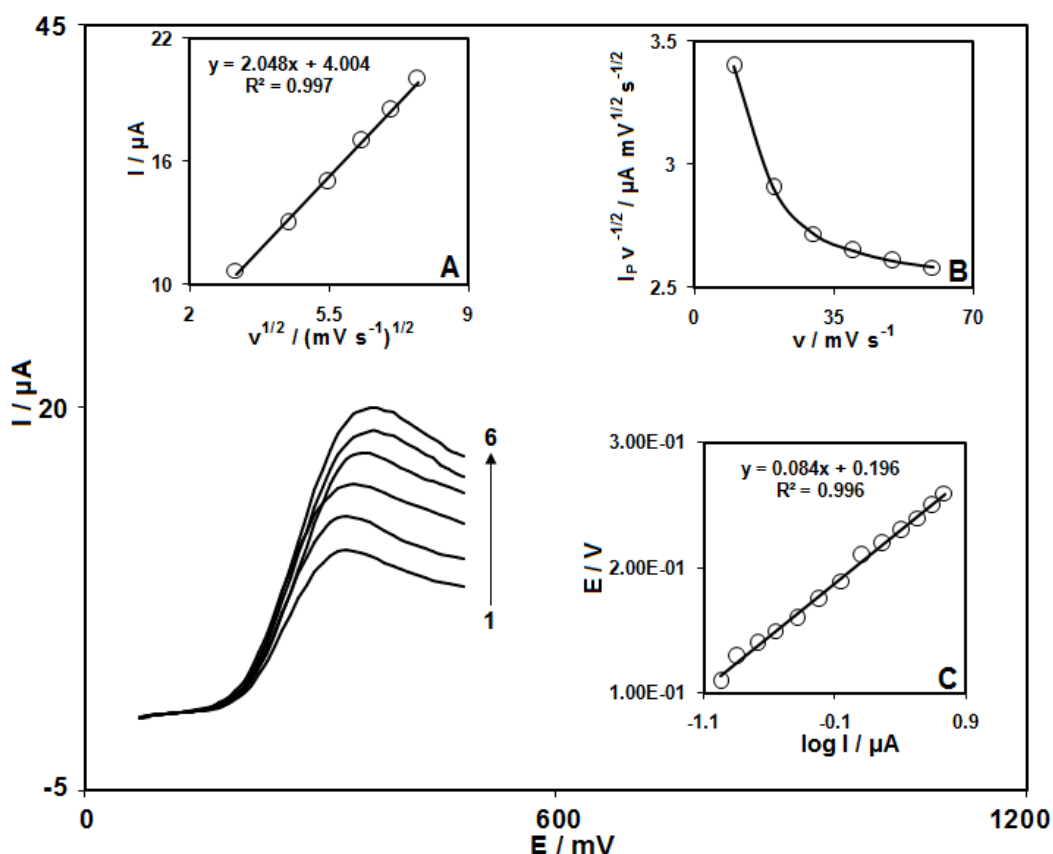


Fig. 4. Linear sweep voltammograms of MC-CNPE in 0.1 M PBS (pH 7.0) containing 100.0 μM AA at various scan rates; From inner to outer scan rates of 10, 20, 30, 40, 50 and 60 mV s^{-1} , respectively. Insets: variation of (A) anodic peak current vs. $v^{1/2}$; (B) normalized current ($I_p/v^{1/2}$) vs. v ; (C) Tafel plot derived from the rising part of the voltammograms recorded at the scan rates of 10 mV s^{-1} .

Chronoamperometry can also be employed to evaluate the catalytic rate constant, k , for the reaction between AA and the MC-CNPE according to the method of Galus [54]:

$$I_C / I_L = \gamma^{1/2} [\pi^{1/2} \text{erf}(\gamma^{1/2}) + \exp(-\gamma) / \gamma^{1/2}] \quad (2)$$

where I_C is the catalytic current of AA at the MC-CNPE, I_L is the limited current in the absence of AA and $\gamma = kC_b t$ is the argument of the error function (C_b is the bulk concentration of AA). In cases where γ exceeds the value of 2, the error function is almost

equal to 1 and therefore, the above equation can be reduced to:

$$I_C / I_L = \pi^{1/2} \gamma^{1/2} = \pi^{1/2} (kC_b t)^{1/2} \quad (3)$$

where t is the time elapsed. The above equation can be used to calculate the rate constant, k , of the catalytic process from the slope of I_C/I_L vs. $t^{1/2}$ at a given AA concentration. From the values of the slopes, the average value of k was found to be $3.62 \times 10^4 \text{ M}^{-1} \text{ s}^{-1}$.

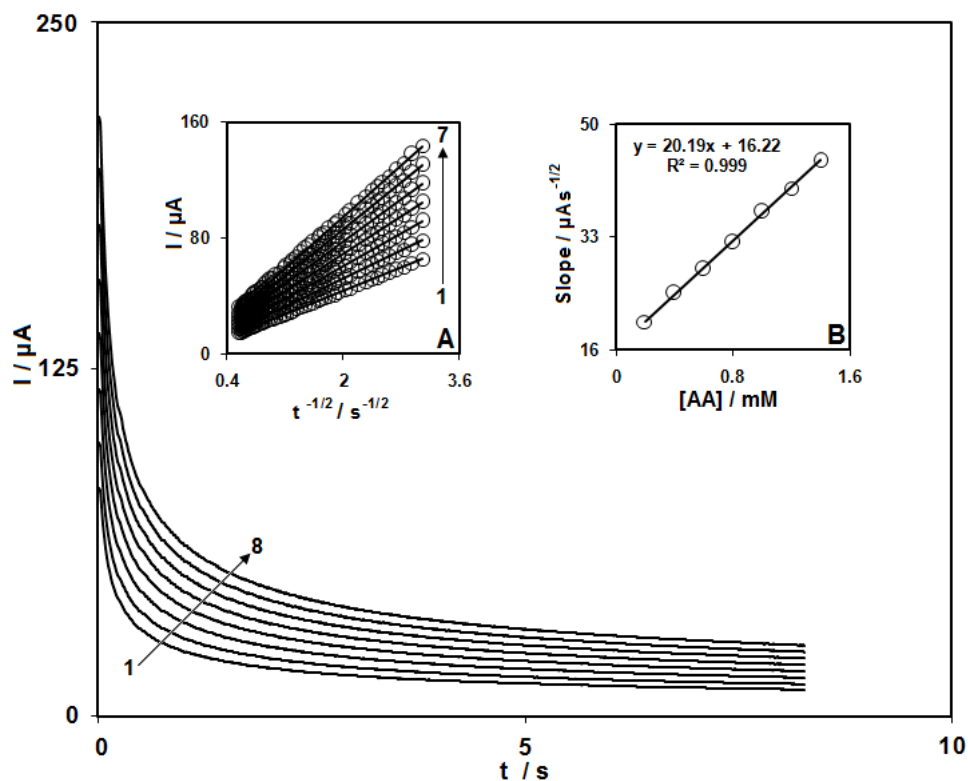


Fig. 5. (A) Chronoamperograms obtained at MC-CNPE in 0.1 M PBS (pH 7.0) for different concentration of AA. The numbers 1–8 correspond to 0.0, 0.2, 0.4, 0.6, 0.8, 1.0, 1.2 and 1.4 mM of AA. Insets: (A) Plots of I vs. $t^{-1/2}$ obtained from chronoamperograms 2–8 (B) Plot of the slope of the straight lines against AA concentration.

3.5. Calibration plot and limit of detection

DPV method was used to determine the concentration of AA. The plot of peak current vs. AA concentration consisted of two linear segments with slopes of 0.2326 and 0.0155 $\mu\text{A } \mu\text{M}^{-1}$ in the concentration ranges of 0.1 to 45.0 μM and 45.0 to 950.0 μM , respectively. The decrease in sensitivity (slope) of the second linear segment is likely due to kinetic limitation. The detection limit (3σ) of AA was found to be 89.0 nM.

3.6. Simultaneous determination of AA and UA

One of the main objectives of the present study was the development of a modified electrode capable of the electro-catalytic oxidation of AA and separation of the electrochemical responses of AA and UA. Therefore, the utilization of the MC-CNPE for the simultaneous determination of AA and UA was demonstrated by simultaneously changing the concentrations of AA and UA (Fig.6).

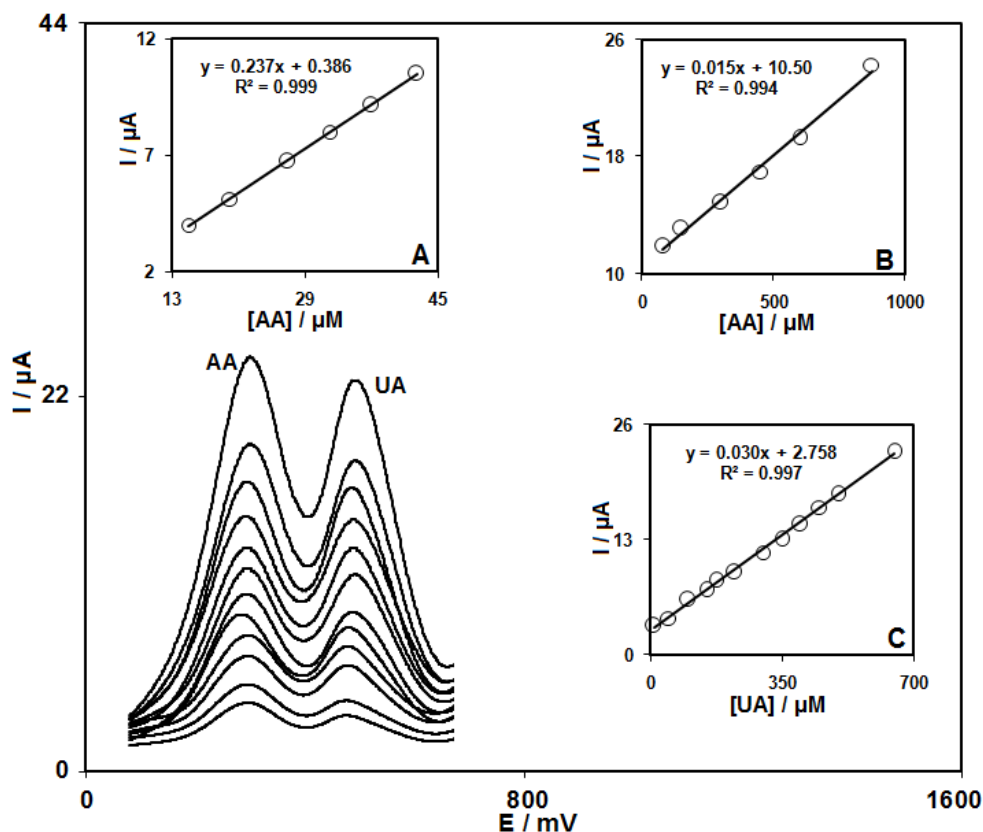


Fig. 6. DPVs of MC-CNPE in 0.1 M PBS (pH 7.0) containing different concentrations of AA+UA in μM , from inner to outer: 15.0+10.0, 20.0+50.0, 27.0+100.0, 32.0+150.0, 37.0+175.0, 42.5+225.0, 80.0+300.0, 150.0+350.0, 300.0+400.0, 450.0+450.0, 600.0+500.0, and 875.0+650.0 respectively. Insets (A), (B) and (C) are plots of I_p vs. AA and UA concentrations, respectively.

The modified electrode displayed strong function for resolving the overlapping voltammetric responses of AA and UA into two well-defined voltammetric peaks with potential differences of 290 mV between AA and UA, which was large enough to determine AA and UA individually and simultaneously.

3.7. Interference study

The influences of various foreign species on the determination of AA was investigated. The tolerance limit was taken as the maximum concentration of the

foreign substances which caused an approximately $\pm 5\%$ relative error in the determination. According to the results, L-lysine, glucose, NADH, acetaminophen, L-asparagine, L-serine, L-threonine, L-proline, histidine, glycine, methionine, tryptophan, phenylalanine, lactose, saccharose, fructose, benzoic acid, methanol, ethanol, urea, Ca^{2+} , Mg^{2+} , Al^{3+} , NH_4^+ , Fe^{+2} , Fe^{+3} , Li^+ , Na^+ , K^+ , Mg^{2+} , F^- , SO_4^{2-} and S^{2-} did not show interference in the determination of AA, but dopamine, norepinephrine and epinephrine showed interferences.

3.8. The repeatability and stability of MC-CNPE

The electrode capability for the generation of a reproducible surface was examined by cyclic voltammetric data obtained in optimum solution pH 7.0 from five separately prepared MC-CNPEs. The calculated RSD for various parameters accepted as the criteria for a satisfactory surface reproducibility (about 1 – 4%), which is virtually the same as that expected for the renewal or ordinary carbon paste surface. However we regenerated the surface of MC-CNPE before each experiment according to our previous results [37].

In addition, the longterm stability of the MC-CNPE was tested over a three-week period. When CVs were recorded after the modified electrode was stored in atmosphere at room temperature, the peak potential for AA oxidation was unchanged and the current signals showed less than 2.6% decrease relative to the initial response. The antifouling properties of the modified electrode toward AA oxidation and its oxidation products were investigated by recording the cyclic voltammograms of the modified electrode before and after use in the presence of AA.

Cyclic voltammograms were recorded in the presence of AA after having cycled the potential 15 times at a scan rate of 10 mV s^{-1} . The peak potentials were unchanged and the currents decreased by less than 2.3 %. Therefore, at the surface of MC-CNPE, not only the sensitivity increase, but the fouling effect of the analyte and its oxidation product also decreases.

3.9. Determination of AA in pharmaceutical sample

The proposed MC-CNPE was found to work well under laboratory conditions. The electrode was also successfully applied to the direct determination of AA content of pharmaceutical samples. The AA content in pharmaceutical samples was determined by the standard addition method in order to prevent of any matrix effect. The results for the analysis of pharmaceutical samples with the voltammetric method compared favorably with those obtained by the USP standard method (Table 2).

4. Conclusion

The MC-CNPE was prepared and used for the investigation of the electrochemical behavior of AA. One pair of well-defined redox peaks were obtained in 0.1 M PBS for MC-CNPE. The MC-CNPE showed excellent electrocatalytic activity for the oxidation of AA.

The DPV currents of AA at MC-CNPE increased linearly with the AA concentration in the range from 0.1 to 950.0 μM with a detection limit of 89.0 nM. The modified electrode exhibited excellent electrocatalytic activity towards the simultaneous detection of AA and UA with wide potential differences. Thus, the electrode could electrochemically discriminate the sensing of AA and UA. Thus, simultaneous as well as independent electrochemical determinations of AA and UA are possible without electrochemical interference from each other. Finally, this method was used for the determination of AA in some pharmaceutical preparations.

Table 2. Determination of AA in real samples

Pharmaceutical preparation	Claimed (mg)	Proposed method [a] (mg)(%RSD)	Iodine methoda (mg; %RSD)	F _{exp.}	T _{exp.}
Effervescent tablet	1000 per tablet	985.0 (0.4)	980.0 (0.3)	1.85	0.8
Ampoule	500 per 5 ml	505.0 (0.3)	497.0 (0.5)	1.2	1.1
Multivitaminic syrup	60 per 5 ml	60.2 (1.3)	59.1 (1.6)	2.1	1.2

^a Result based on five replicate determinations per samples. Theoretical values for $t=2.31$ and $F=6.39$ ($p=0.05$)

5. References

- [1] H.K. Choi, X. Gao, G. Curhan, Arch. Intern. Med., 169 (2009) 502.
- [2] D.T. Alexandrescu, C.A. Dasanu, C.L. Kauffman, Clin. Exp. Dermatol., 34 (2009) 811.
- [3] M.C. Polidori, W. Stahl, O. Eichler, I. Niestroj, H. Sies, Free Radical Biol. Med. 30 (2001) 456.
- [4] M.H. Alderman, Curr. Opin. Pharmacol., 2 (2002) 126.
- [5] G.C. Curhan, E.N. Taylor, J. Urol., 181 (2009) 1721.
- [6] H.A. Jinnah, Dis. Models Mech., 2 (2009) 116.
- [7] Y. Zhao, X. Yang, W. Lu, H. Liao, F. Liao, Microchim. Acta, 164 (2009) 1.
- [8] S.L. Feng, J. Wang, X.G. Chen, J. Fan, Spectrochim. Acta, Part A 61 (2005) 841.
- [9] Z. Gazdik, O. Zitka, J. Petrlova, V. Adam, J. Zehnalek, A. Horna, V. Reznicek, M. Beklova, R. Kizek, Sensors, 8 (2008) 7097.
- [10] J. B. Raof, R. Ojani, H. Beitollahi, R. Hossienzadeh, Electroanalysis, 18 (2006) 1193.
- [11] D. Zheng, J. Ye, L. Zhou, Y. Zhang, C. Yu, J. Electroanal. Chem., 625 (2009) 82.
- [12] H. Beitollahi, M. Mazloum Ardakani, H. Naeimi, B. Ganjipour, J. Solid State Electrochem., 13 (2009) 353.
- [13] F. Sekli-Belaidi, P. Temple-Boyer, P. Gros, J. Electroanal. Chem., 647 (2010) 159.
- [14] R. Manjunatha, G. Shivappa Suresh, J. S. Melo, S.F. D'Souza, T. V. Venkateshac, Sens. Actuators B, 145 (2010) 643.
- [15] P. Kalimuthu, S. A. John, Talanta, 80 (2010) 1686.
- [16] B. Habibi, M. H. Pournaghi-Azarb, Electrochim. Acta, 55 (2010) 5492.
- [17] S. Thiagarajan, T.H. Tsai, S.M. Chen, Biosens. Bioelectron., 24 (2009) 2712.
- [18] S. Zhang, M. Xu, Y. Zhang, Electroanalysis, 21 (2009) 2607.
- [19] S.A. Kumar, H.-W. Cheng, S.-M. Chen, Electroanalysis, 21 (2009) 2281.
- [20] P. Kalimuthu, S.A. John, Bioelectrochemistry, 77 (2009) 13.
- [20] M.E. Rice, Z. Galus, R.N. Adams, J. Electroanal. Chem., 143 (1983) 89.
- [21] J.B. Raof, R. Ojani, H. Beitollahi, Electroanalysis, 19 (2007) 1822.
- [22] J. Wang, N. Naser, L. Angnes, H. Wu, L.G. Chen, Anal. Chem., 64 (1992) 1285.
- [23] J.B. Raof, R. Ojani, H. Beitollahi, R. Hosseinzadeh, Anal. Sci., 22 (2006) 1213.
- [24] K. Kalcher, Electroanalysis, 2 (1990) 419.

- [25] H. Beitollahi, I. Sheikhshoaieb, *Electrochim. Acta*, 56 (2011) 10259.
- [26] R.N. Adams, *Anal. Chem.*, 30 (1958) 1576.
- [27] J.V.B. Kozan, R.P. Silva, S.H.P. Serrano, A.W.O. Lima, L. Angnes, *Anal. Chim. Acta*, 591 (2007) 200.
- [28] H. Karimi-Maleh, M. Keyvanfard¹, K. Alizad, M. Fouladgar, H. Beitollahi, A. Mokhtari, F. Gholami-Orimi, *Int. J. Electrochem. Sci.*, 6 (2011) 6141.
- [29] H. Beitollahi, J.B. Raof, R. Hosseinzadeh, *Talanta*, 85 (2011) 2128.
- [30] M. Muti, A. Erdem, A. Caliskana, A. Sinag, T. Yumak, *Colloids Surf. B*, 86 (2011) 154.
- [31] H. Beitollahi, I. Sheikhshoaie, *J. Electroanal. Chem.*, 661 (2011) 336.
- [32] Z. Lin, J. Sun, J. Chen, L. Guo, Y. Chen, G. Chen, *Anal. Chem.*, 80 (2008) 2826.
- [33] J.B. Raof, R. Ojani, H. Beitollahi, *Int. J. Electrochem. Sci.*, 2 (2007) 534.
- [34] M.A. Kamyabi, Z. Asgari, H.H. Monfared, A. Morsali, *J. Electroanal. Chem.*, 632 (2009) 170.
- [35] J. Raof, A. Omrani, R. Ojani, F. Monfared, *J. Electroanal. Chem.*, 633 (2009) 639.
- [36] S. Shahrokhian, M. Ghalkhani, M.K. Amini, *Sens. Actuators B*, 137 (2009) 669.
- [37] H. Beitollahi, I. Sheikhshoaie, *Anal. Methods*, 3 (2011) 1810.
- [38] M.B. Fritzen-Garcia, I. Rosane, W.Z. Oliveira, B.G. Zanetti-Ramos, O. Fatibello-Filho, V. Soldi, A.A. Pasa, T.B. Creczynski-Pasa, *Sens. Actuators B*, 139 (2009) 570.
- [39] H. Mahmoudi Moghaddam, H. Beitollahi, *Int. J. Electrochem. Sci.*, 6 (2011) 6503.
- [40] J. Tashkhourian, M.R. Hormozi Nezhad, J. Khodavesi, S. Javadi, *J. Electroanal. Chem.*, 633 (2009) 85.
- [41] H. Beitollahi, I. Sheikhshoaie, *Mater. Sci. Eng. C*, 32 (2012) 375.
- [42] S. Iijima, *Nature*, 354 (1991) 56.
- [43] F. Berti, L. Lozzi, I. Palchetti, S. Santucci, G. Marrazza, *Electrochim. Acta*, 54 (2009) 5035.
- [44] H. Beitollahi, H. Karimi-Maleh, H. Khabazzadeh, *Anal. Chem.*, 80 (2008) 9848.
- [45] J. Wang, *Electroanalysis*, 17 (2005) 7.
- [46] H. Beitollahi, J.B. Raof, R. Hosseinzadeh, *Electroanalysis*, 23 (2011) 1934.
- [47] J. Huang, Y. Liu, H. Hou, T. You, *Biosens. Bioelectron.*, 24 (2008) 632.
- [48] H. Beitollahi, J.B. Raof, H. Karimi-Maleh, R. Hosseinzadeh, *J. Solid State Electrochem.*, 16 (2012) 1701.
- [49] G. Hu, Y. Ma, Y. Guo, S. Shao, *Electrochim. Acta*, 53 (2008) 6610.
- [50] H. Beitollahi, J.B. Raof, R. Hosseinzadeh, *Anal. Sci.*, 27 (2011) 991.
- [51] I. Sheikhshoaie, A. Rezaeifard, N. Monadi, S. Kaafi, *Polyhedron* 28 (2009) 733.
- [52] A.J. Bard, L.R. Faulkner, *Electrochemical Methods: Fundamentals and Applications*, 2nd ed. Wiley, New York, 2001.
- [53] E. Laviron, *J. Electroanal. Chem.* 101 (1979) 19.
- [54] Z. Galus, *Fundamentals of Electrochemical Analysis*, Ellis Horwood, New York, 431, 1976.